# Electronic Supplementary Information

# Photoelectrochemical $CO_2$ Reduction to Adjustable Syngas on Grain-boundary-mediated a-Si/$TiO_2$/Au Photocathodes with Low Onset Potentials

Chengcheng Li,[a] Tuo Wang,[a] Bin Liu,[a] Mengxin Chen,[a] Ang Li,[a] Gong Zhang,[a] Minyong Du,[b] Hui Wang,[b] Shengzhong Frank Liu[b] and Jinlong Gong*[a]

[a.] *Key Laboratory for Green Chemical Technology of Ministry of Education, School of Chemical Engineering and Technology, Tianjin University; Collaborative Innovation Center of Chemical Science and Engineering (Tianjin), Tianjin 300072, China*

[b.] *iChEM, Dalian Institute of Chemical Physics, Dalian National Laboratory for Clean Energy, Chinese Academy of Sciences, Dalian 116023, China*

* Corresponding authors: jlgong@tju.edu.cn; Fax: +86-22-87401818

## Experimental Section

### The fabrication of a-Si photocathodes

FTO glass substrates were cleaned in ultra-sonic with acetone/isopropanol/ethanol/DI water, sequentially. The a-Si photocathodes with a sandwich structure of p-i-n were deposited at 200 °C onto FTO by a multi-chamber cluster PECVD apparatus, where the p-type, n-type and intrinsic layers were deposited in separated chambers to avoid cross-contamination. The growth sequence was (1) two layers of p-type amorphous silicon with a p-type nanocrystalline silicon between these two, with a total thickness of 15 nm, (2) 650 nm of intrinsic amorphous silicon as the active light absorber material, (3) 30 nm n-type nanocrystalline silicon.

### The deposition of $TiO_2$ protective layer

40 nm of amorphous $TiO_2$ was deposited onto the above a-Si photocathodes at 150 °C in a custom-made ALD system, using Titanium(IV) isopropoxide (TTIP, Sigma-Aldrich, ≥99.9999%) and ultrapure water as precursors. The precursors were held at 65 °C and 25 °C, respectively. The pressure was held at 1 torr during deposition. One ALD cycle consists of TTIP dose for 1 s, $N_2$ purge for 10 s, water dose for 0.1 s and $N_2$ purge for 10 s. The growth per cycle for $TiO_2$ is 0.3 Å/cycle.

### The deposition of Au catalytic layer

2, 4, 7, 11 and 20 nm of Au catalytic layers were deposited onto a-Si/$TiO_2$ using an e-beam evaporator at a deposition rate of 1 nm/min. The resultant a-Si/$TiO_2$/Au samples are denoted as ST-2Au, ST-Au, ST-7Au, ST-11Au and ST-20Au, respectively.

### Characterization

The morphology was characterized by field emission scanning electron microscope (FE-SEM, Hitachi S-4800, 5kV) and transmission electron microscope (TEM, JEOL JEM-2100F, 200 kV). XPS analysis of the samples was carried out on a Physical Electronics PHI 1600 ESCA system with an Al Kα X-ray source (1486.6 eV). The binding energy was calibrated using the C 1s photoelectron peak at 284.6 eV as the reference.

The thickness of ALD-$TiO_2$ on monocrystalline Si monitor substrate was obtained from spectroscopic ellipsometry (M-2000 DI, J.A. Woollam Co., Inc.) at 60° and 70° incident angle, by fitting the amplitude ratio (Ψ) and phase shift (Δ) of polarized light with the Cauchy dispersion model. The Si monitor substrate was placed 10 mm next to the a-Si sample in the same batch. Structure of this optical model:

| | |
|---|---|
| Layer 2 | $TiO_2$ (Cauchy model) |
| Layer 1 | Native oxide (1.8 nm, measured before deposition) |
| Substrate | Monocrystalline Si |

Fitting results: $TiO_2$ thickness = 41.1 nm (1300 cycles) with MSE = 5.81. MSE refers to mean squared error. This thickness is equal to the result of cross-sectional SEM (Fig. S1b), because the nucleation and growth of $TiO_2$ is nearly identical on the surface of a-Si and monocrystalline Si substrates.

**PEC $CO_2$ reduction**

PEC $CO_2$ reduction was performed in $CO_2$-saturated 0.1 M $KHCO_3$ solution (pH 6.8) in a conventional H-cell (separated by Nafion 115) under 25 °C and 1 bar, using a three-electrode configuration with a-Si/$TiO_2$/Au electrodes (encapsulated with epoxy) as the working electrodes, saturated Ag/AgCl as the reference electrode, and a platinum foil (2 × 2 $cm^2$) as the counter electrode. During PEC measurements, a-Si/$TiO_2$/Au electrodes were irradiated by a 300 W xenon lamp (Beijing Perfectlight Technology Co. Lt, LS-SXE300CUV) equipped with an AM 1.5G filter. The intensity of the light was adjusted to 100 mW $cm^{-2}$. An electrochemical workstation (CompactStat.e20250, IVIUM) was used to measure the current-potential (*J-V*)

curves and chronoamperometry. *J-V* curves were performed at a scan rate of 50 mV/s. All potentials of photoelectrodes in this paper were reported versus RHE:

$$V_{\mathrm{RHE}} = V_{\mathrm{AgCl}} + 0.197(\mathrm{V}) + 0.059pH \quad (1)$$

The effective areas of the electrodes were calculated by Image software.

The reactor cell was linked to a gas chromatography (Ruimin GC 2060, Shanghai) for on-line test. $H_2$ and $CO_2$ were detected by TCD and CO was detected by FID equipped with a methanizer. Under the reaction conditions, only CO and $H_2$ were detected by gas chromatography, and the total FEs of CO and $H_2$ were about 100%.

The possible liquid products were analyzed by AVANCE III HD 400 MHz NanoBAY (Bruker). A 0.5-mL sample of the electrolyte was mixed with 0.1 mL $D_2O$ (5 mM dimethyl sulphoxide). Dimethyl sulphoxide (DMSO, Sigma, 99.99%) was added as an internal standard. The one-dimensional $^1$H spectrum was measured with water suppression mode (Fig. S7).

The half-cell efficiency, or the applied bias photon-to-current efficiency (ABPE) was calculated using the following equation:

$$\eta(\%) = \left[\frac{J(\mathrm{mA{\cdot}cm^{-2}}) \times \mathrm{FE_{CO}}(\%) \times (1.34 - V_{\mathrm{bias}})(\mathrm{V}) + J(\mathrm{mA{\cdot}cm^{-2}}) \times \mathrm{FE_{H2}}(\%) \times (1.23 - V_{\mathrm{bias}})}{P_{\mathrm{in}}(\mathrm{mW{\cdot}cm^{-2}})}\right] \quad (2)$$

where $J$ is the photocurrent density of a-Si/$TiO_2$/Au photocathodes, $FE_{CO}$ and $FE_{H2}$ are Faradaic efficiency towards CO and $H_2$ respectively, $V_{\mathrm{bias}}$ is the applied potential versus an ideal counter electrode for $O_2$ evolution (1.23 V *vs.* RHE), and $P_{\mathrm{in}}$ is the light intensity (100 mW $cm^{-2}$).

The unassisted overall solar-to-syngas efficiency $\eta_{\mathrm{sts}}$ was calculated using the following equation:

$$\eta_{\mathrm{sts}}(\%) = \left[\frac{J(\mathrm{mA{\cdot}cm^{-2}}) \times \mathrm{FE_{CO}}(\%) \times 1.34(\mathrm{V}) + J(\mathrm{mA{\cdot}cm^{-2}}) \times \mathrm{FE_{H2}}(\%) \times 1.23(\mathrm{V})}{P_{\mathrm{in}}(\mathrm{mW{\cdot}cm^{-2}})}\right] \quad (3)$$

Where $J$ is the unbiased photocurrent density.

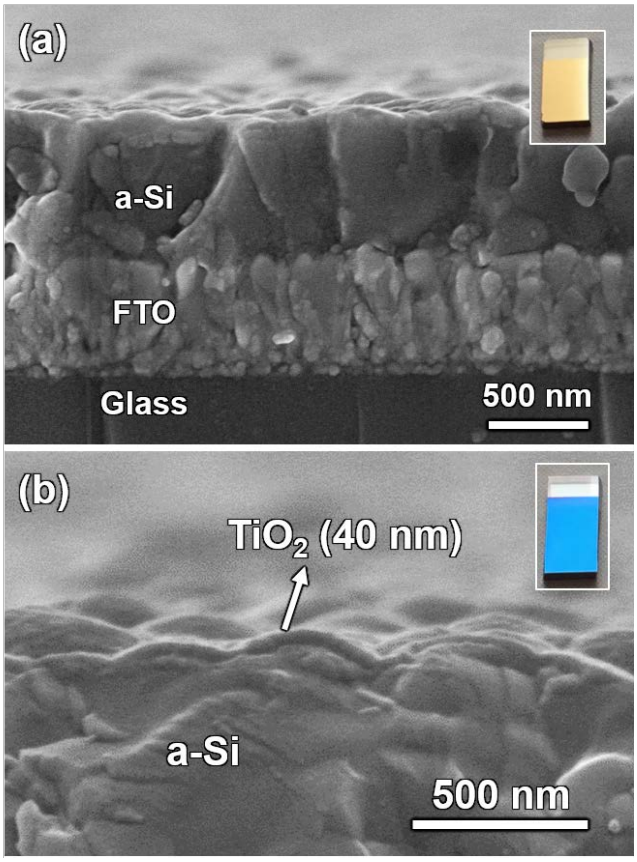


**Fig. S1** Cross-sectional SEM images of (a) a-Si and (b) a-Si/$TiO_2$ electrodes. The insets show the sample photographs.

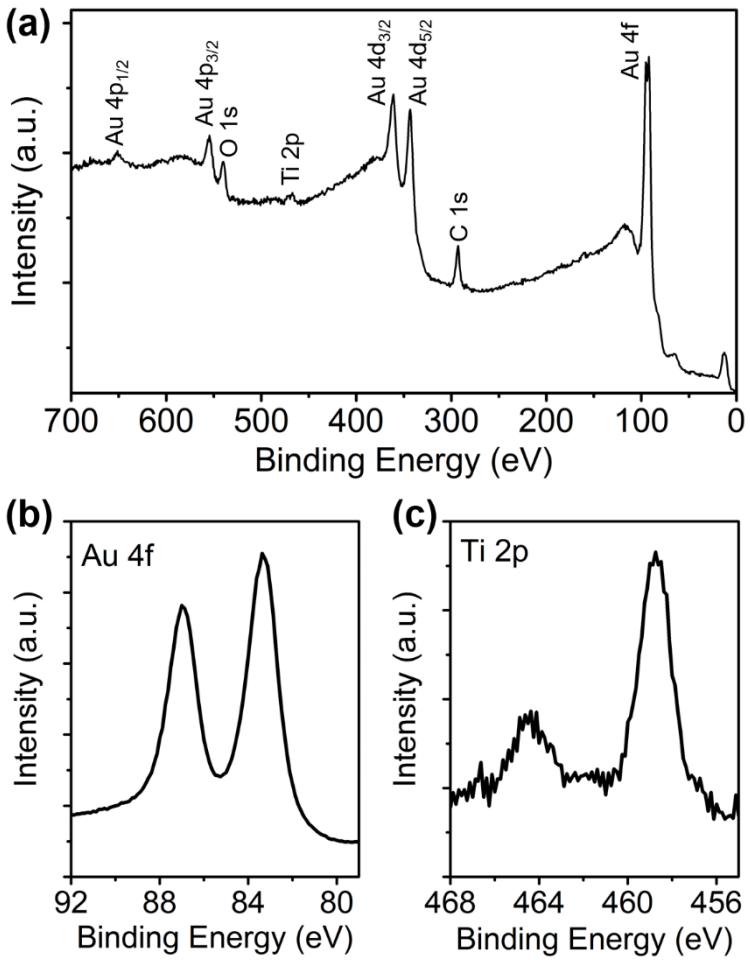


**Fig. S2** XPS of ST-7Au electrode. (a) XPS survey spectrum. (b, c) High-resolution XPS spectra of the Au 4f and Ti 2p.

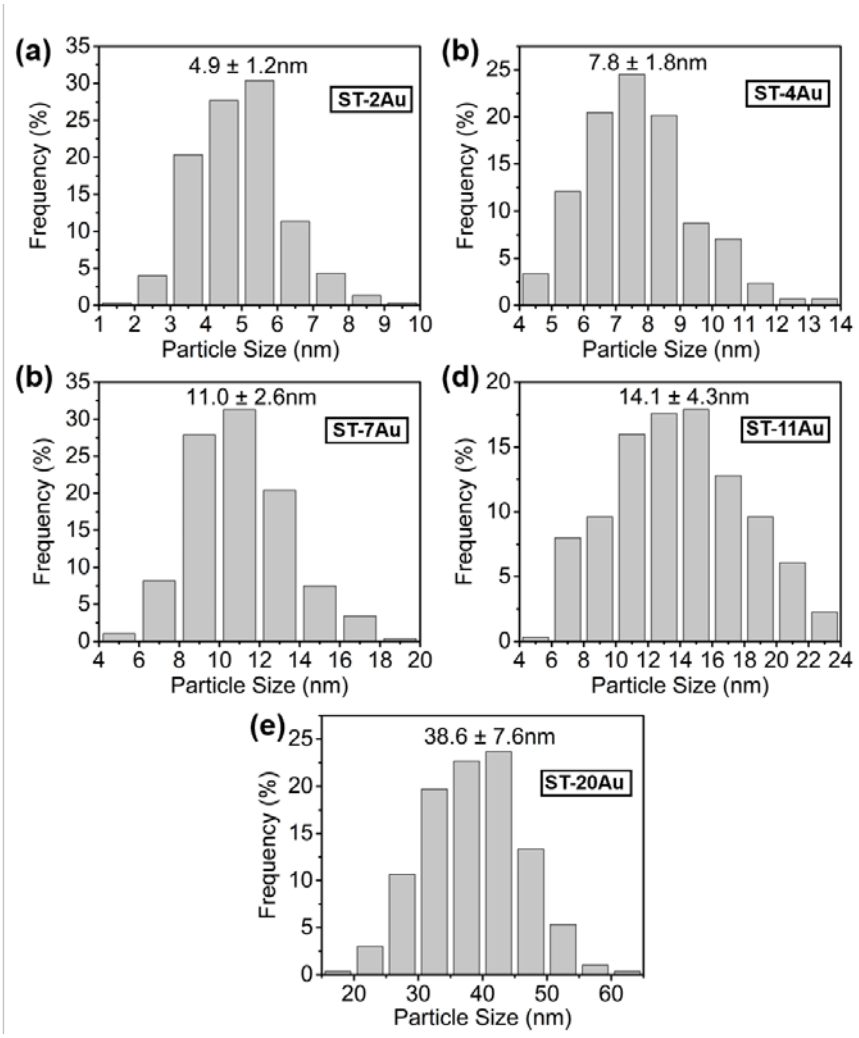


**Fig. S3** Au particle size distributions of different a-Si/$TiO_2$/Au samples: (a) ST-2Au, (b) ST-4Au, (c) ST-7Au, (d) ST-11Au and (e) ST-20Au. The distributions were obtained by counting 300 particles from TEM in each sample.

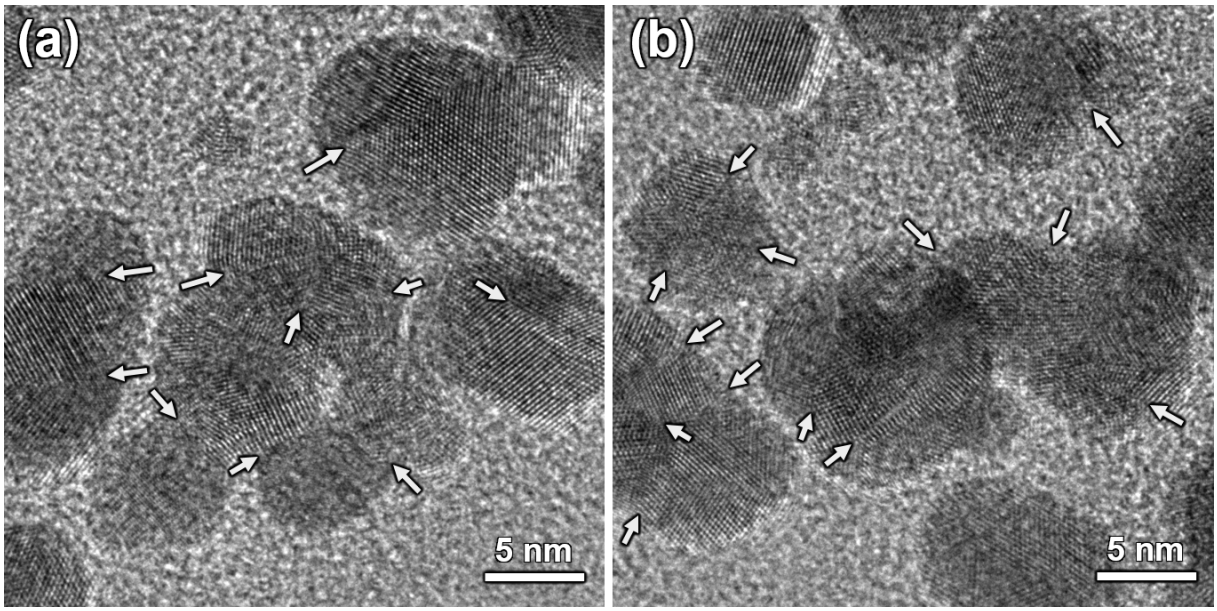


**Fig. S4** Additional TEM images of Au NPs for ST-4Au showing that most of the Au NPs are polycrystalline with rich GBs. The arrows indicate GBs in the NPs.

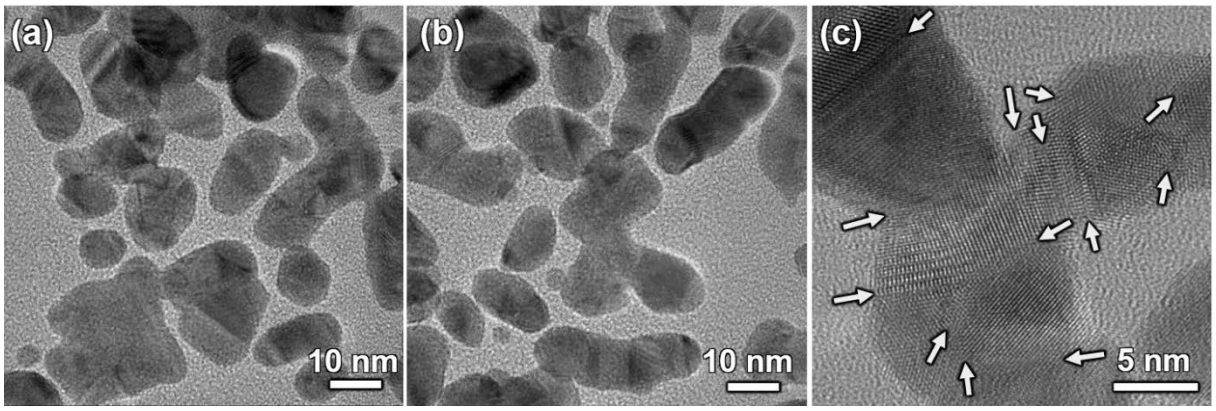


**Fig. S5** Additional TEM images of Au NPs for ST-7Au, showing that cross-linking between NPs provide additional GBs. The arrows in (c) indicate GBs.

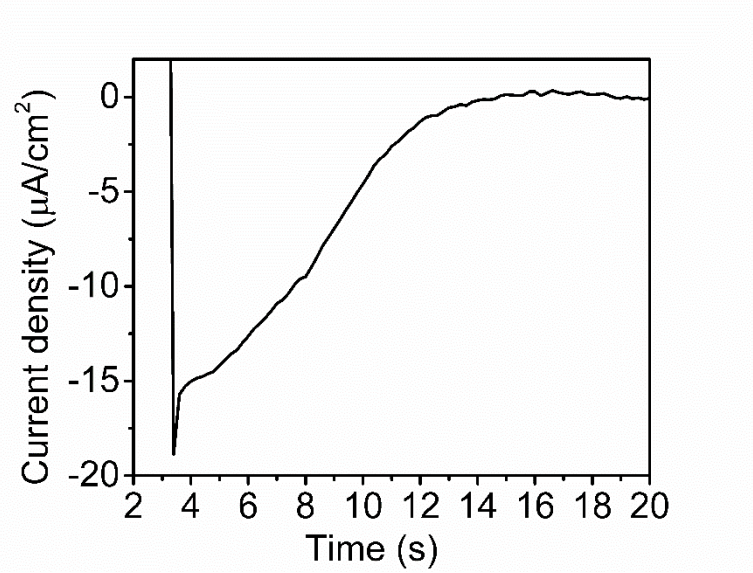


**Fig. S6** Chronoamperometry of bare a-Si photocathode without $TiO_2$ protective layer in $CO_2$-saturated 0.1 M $KHCO_3$ at −0.1 $V_{RHE}$ under simulated 1 sun illumination.

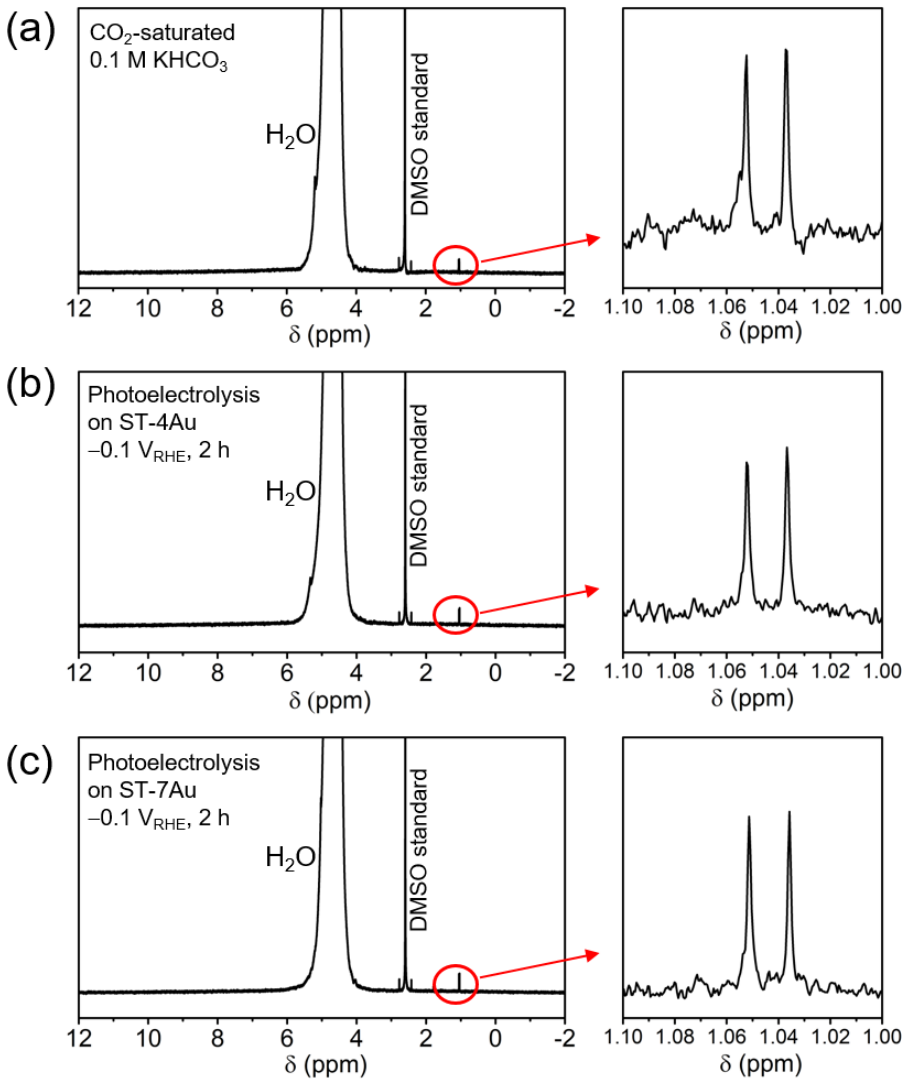


**Fig. S7** Representative $^{1}$H-NMR spectra obtained from the electrolyte after reactions. DMSO (Dimethyl sulphoxide) is used as an internal standard. (a) $CO_2$-saturated 0.1 M $KHCO_3$ electrolyte without photoelectrolysis reaction. (b) Photoelectrolysis by ST-4Au (–0.1 $V_{RHE}$, 2 h). (c) Photoelectrolysis by ST-4Au (–0.1 $V_{RHE}$, 2 h).

There are no liquid products detected from NMR spectra. The two peaks around 1.05 are not attributed to any liquid products, and are also observed from unreacted electrolyte (Fig. S7a). They might come from DMSO agents.

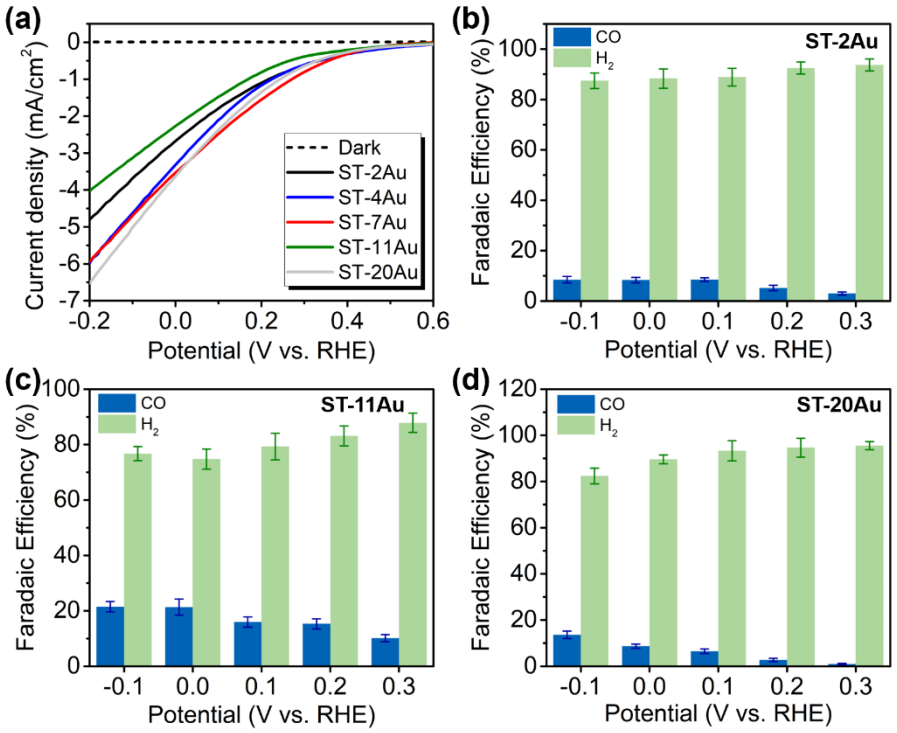


**Fig. S8** (a) PEC *J*-*V* curves for different a-Si/$TiO_2$/Au samples in $CO_2$-saturated 0.1 M $KHCO_3$ electrolyte (pH 6.8) under simulated 1 sun illumination. (b-d) Faradaic efficiency toward CO and $H_2$ as a function of potential for ST-2Au, ST-11Au and ST-20Au electrodes.

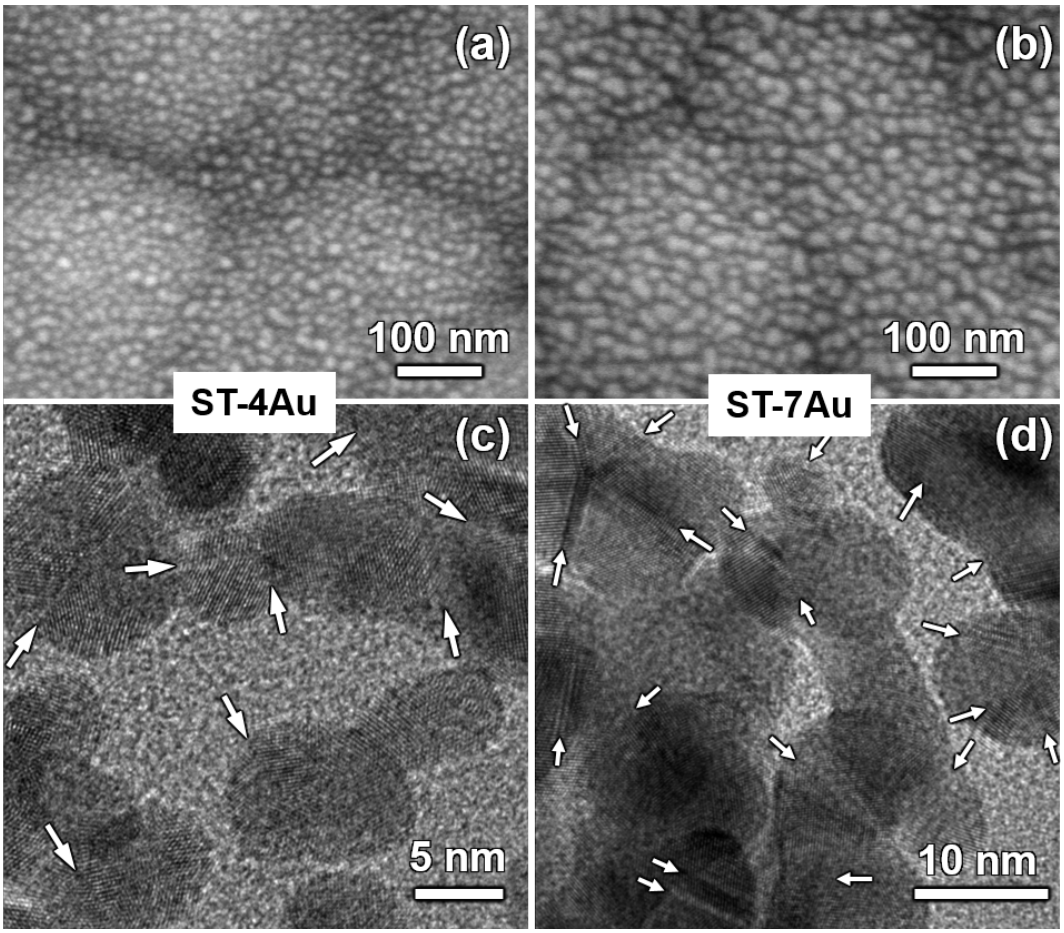


**Fig. S9** Planar SEM (a-b) and Au TEM (c-d) images for ST-4Au (a,c) and ST-7Au (b,d) electrodes after PEC stability tests at −0.1 $V_{RHE}$ for 10 h. The arrows indicate GBs.

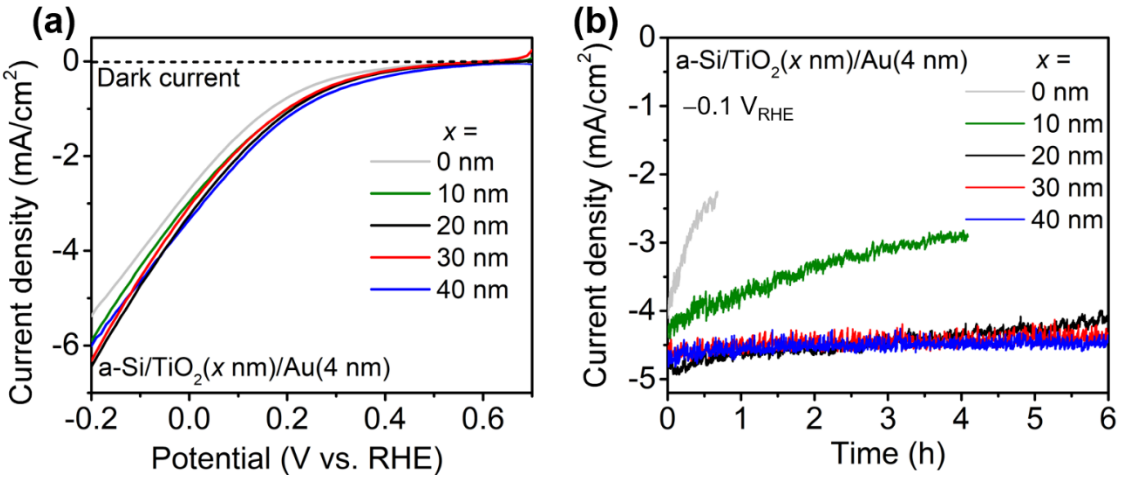


**Fig. S10** Effect of $TiO_2$ thickness on the performance of a-Si/$TiO_2$/Au photocathodes. (a) PEC *J*-*V* curves for different a-Si/$TiO_2$(*x* nm)/Au(4 nm) samples. The thickness of $TiO_2$ varies from 0 to 40 nm. (b) Respective PEC stability tests of a a-Si/$TiO_2$(*x* nm)/Au(4 nm) samples at –0.1 $V_{RHE}$. Both (a) and (b) were measured in $CO_2$-saturated 0.1 M $KHCO_3$ electrolyte (pH 6.8) under simulated 1 sun illumination.

The thickness of $TiO_2$ has little effect on the photocurrent values (Fig. S10a), but has a great impact on the photoelectrode stability (Fig. S10b). The photoactivity of a-Si/Au (4 nm) without $TiO_2$ protective layer degrades quickly with time. In comparison, the stability of a-Si/$TiO_2$(*x* nm)/Au(4 nm) samples becomes better when $TiO_2$ is thicker. When the thickness of $TiO_2$ achieves 30 nm, there is no observable decrease of photoactivity within 6 h. To guarantee the stability of photoelectrodes and simultaneously save the process time of film deposition, we choose 40 nm as the optimized thickness for $TiO_2$ protective layer.

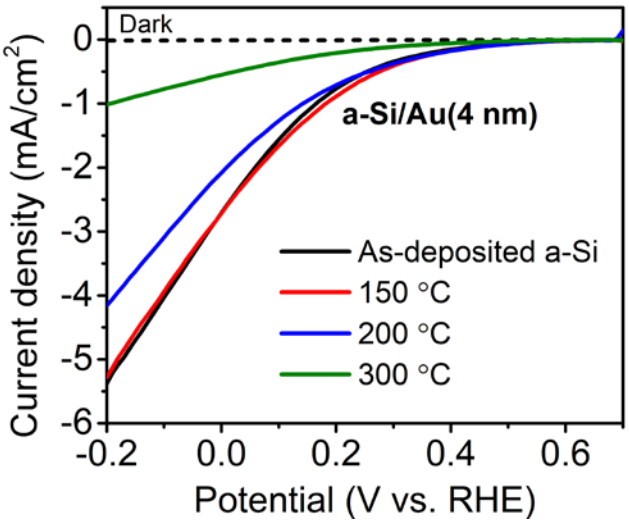


**Fig. S11** Impact of temperature on the performance of a-Si photocathodes. Before Au deposition, a-Si samples were treated at different temperatures (150, 200, 300 °C) in ALD chamber (1 torr) for 8 h, with $N_2$ flowing but no deposition. As-deposited a-Si refers to non-treated sample before Au deposition. The *J-V* curves were measured in $CO_2$-saturated 0.1 M $KHCO_3$ electrolyte (pH 6.8) under simulated 1 sun illumination.

As shown in Fig. S11, 150 °C (ALD deposition temperature) has nearly no effect on the performance, while elevated temperatures (higher than 200 °C) could harm the performance of a-Si photocathodes.

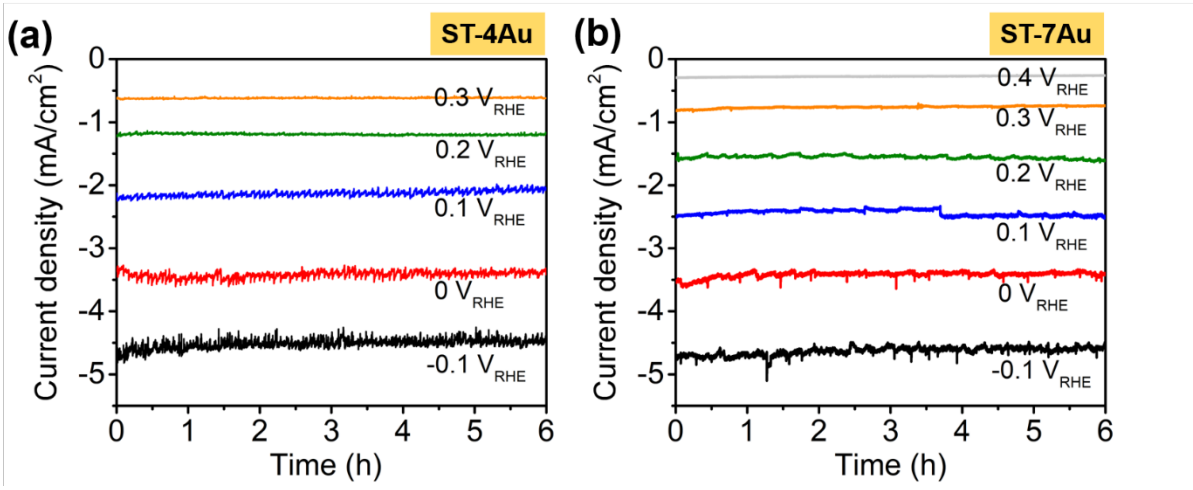


**Fig. S12** Time-dependent photocurrents of ST-4Au (a) and ST-7Au (b) at different potentials in $CO_2$-saturated 0.1 M $KHCO_3$ under simulated 1 sun illumination.

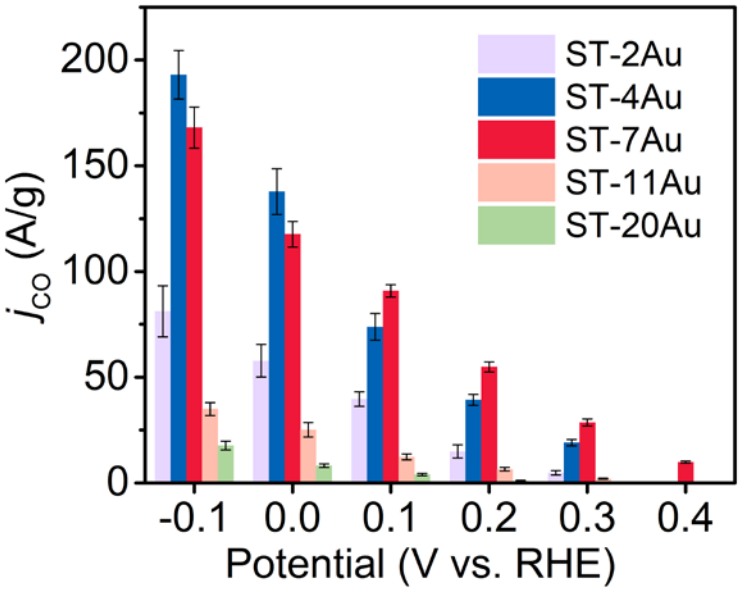


**Fig. S13** CO mass activity (in A/g) of various a-Si/$TiO_2$/Au samples.

The CO mass activity (A/g) values were calculated through dividing partial current density of CO (mA $cm^{-2}$) by Au mass per area (mg $cm^{-2}$). Because quartz crystal monitor (QCM) uses the piezoelectric effect of the quartz crystal to reflect the mass change, the obtained average thickness of Au (density: 19.32g $cm^{-3}$) can be converted to Au mass per area: $1.932\times10^{-3}$ mg $cm^{-2}$ per nanometer of Au.

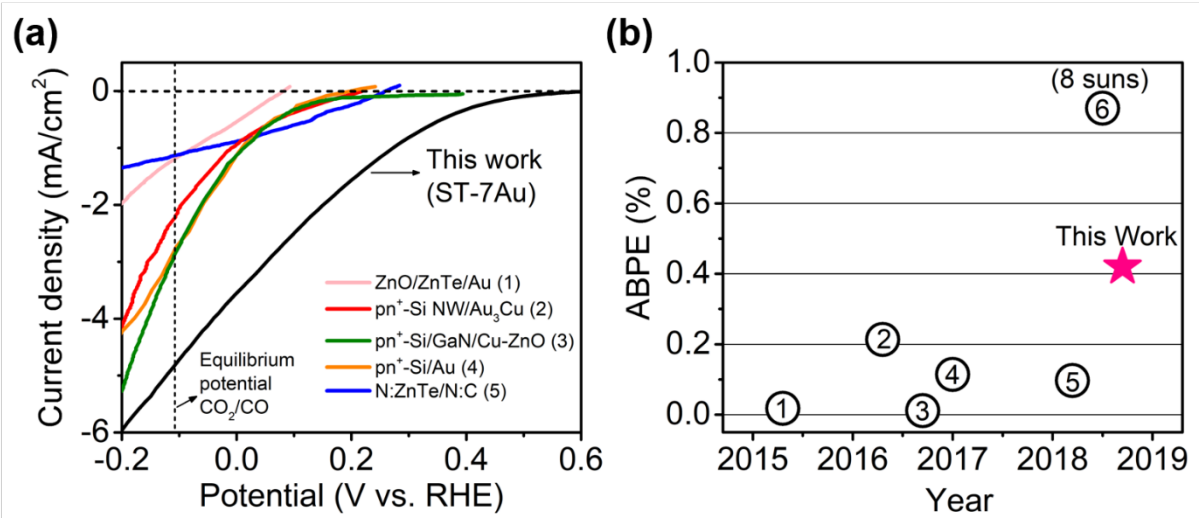


**Fig. S14** Comparison of PEC $CO_2$ reduction performance of our photocathode (ST-7Au) with other representative photocathodes in the literature.[1-6] The numbers in a and b refer to the Reference (Ref.) number. Light intensity in this work and Ref. 1, 4, 5 is the same one sun (100 mW cm$^{-2}$). Light intensity in Ref. 3 and 6 is eight suns (800 mW cm$^{-2}$). Light intensity in Ref. 2 is 20 mW cm$^{-2}$ of 740 nm illumination (comparable to 1/3 sun).

(a) *J*-*V* curves of various photocathodes. Both the onset potential and photocurrent of ST-7Au in this work surpass other photocathodes by a large margin.

(b) Progress in ABPE of photocathodes for aqueous PEC $CO_2$ reduction. Efficiency values were calculated using equation 2 in Experimental section of Supporting Information.

**Table S1** Performance comparison of photocathodes for PEC $CO_2$ reduction in aqueous media.

| Photocathode | Light intensity (sun) | Onset potential ($V_{RHE}$) | ABPE | Ref |
|---|---|---|---|---|
| ZnO/ZnTe/Au | 1 | 0.1 | 0.018% | 1 |
| $pn^+$-Si NW/$Au_3Cu$ | 1/3 | 0.15 | 0.21% | 2 |
| $pn^+$-Si/GaN/Cu-ZnO | 8 | 0.1 | 0.011% | 3 |
| $pn^+$-Si/Au | 1 | 0.2 | 0.11% | 4 |
| N:ZnTe/N:C | 1 | 0.25 | 0.097% | 5 |
| $pn^+$-Si/GaN/Pt-$TiO_2$ | 8 | 0.47 | 0.87% | 6 |
| **a-Si/$TiO_2$/GB-Au (ST-7Au)** | **1** | **0.4** | **0.42%** | **This work** |

1. Y. J. Jang, J.-W. Jang, J. Lee, J. H. Kim, H. Kumagai, J. Lee, T. Minegishi, J. Kubota, K. Domen and J. S. Lee, *Energy Environ. Sci.*, 2015, **8**, 3597-3604.
2. Q. Kong, D. Kim, C. Liu, Y. Yu, Y. Su, Y. Li and P. Yang, *Nano Lett.*, 2016, **16**, 5675-5680.
3. S. Chu, S. Fan, Y. Wang, D. Rossouw, Y. Wang, G. A. Botton and Z. Mi, *Angew. Chem. Int. Ed.*, 2016, **55**, 14262-14266.
4. J. T. Song, H. Ryoo, M. Cho, J. Kim, J.-G. Kim, S.-Y. Chung and J. Oh, *Adv. Energy Mater.*, 2017, **7**, 1601103.
5. Y. J. Jang, M. D. Bhatt, J. Lee, S. H. Choi, B. J. Lee and J. S. Lee, *Adv. Energy Mater.*, 2018, **0**, 1702636.
6. S. Chu, P. Ou, P. Ghamari, S. Vanka, B. Zhou, I. Shih, J. Song and Z. Mi, *J. Am. Chem. Soc.*, 2018, **140**, 7869-7877.